# Spin-flop coupling and rearrangement of bulk antiferromagnetic spins in epitaxial exchange-biased Fe/MnPd/Fe/IrMn multilayers

Wei Zhang and Kannan M. Krishnan*

*Department of Materials Science and Engineering, University of Washington, Seattle, Washington 98195, USA*

(Received 18 April 2012; revised manuscript received 11 June 2012; published 13 August 2012)

The role of bulk antiferromagnetic spins on exchange bias was investigated in interface spin-flop coupled Fe/MnPd bilayers and Fe/MnPd/Fe/IrMn multilayers. Magnetic measurement of the bilayers showed that the exchange bias saturated at a uniquely large critical thickness, ~300 Å, with a spin reorientation transition simultaneously observed. Field cooling of the multilayer, with parallel or antiparallel alignment of the two Fe layers leads to a different MnPd internal spin arrangement. Minor loop studies showed that nonrecoverable changes in the spin structure of the antiferromagnet occurred during the Fe layer reversal. The possibility of manipulating exchange bias of the Fe/MnPd couple by modifying the MnPd bulk spin configuration using the magnetizing process of the Fe/IrMn couple is demonstrated. A qualitative model based on interface spin-flop coupling is proposed to explain all the relevant properties, including the temperature dependence of the exchange bias.

DOI: 10.1103/PhysRevB.86.054415 PACS number(s): 75.70.Cn, 75.60.Jk, 75.30.Gw

## I. INTRODUCTION

The exchange bias (EB) effect,[1] observed for a ferromagnet (FM) in contact with an antiferromagnet (AFM) has attracted much fundamental and technological interest.[2–4] Previous models used to describe the EB effect usually assumed an uncompensated AFM surface and a collinear FM/AFM exchange coupling at the interface.[5] However, micromagnetic calculations show that due to the spin-flop coupling the ground state for a compensated FM/AFM interface is an orthogonal magnetic orientation of the FM and AFM spins.[6–8] Recently, Zhan *et al.*[9] reported an in-plane magnetization reorientation transition, due to spin-flop coupling in Fe/*a* axis MnPd epitaxial EB bilayers, that is driven either by the temperature or the thickness of the AFM layer. A uniaxial anisotropy, $K_u$, perpendicular to the EB, was found induced by the interface. In addition, many recent studies also indicated that the AFM bulk spins play important roles in defining the EB phenomenon.[10–15] Field-cooling experiments[16] also suggested the importance of bulk AFM spin configuration set by the initial FM spin structures.[17] However, the effect of the AFM bulk magnetic structure on the spin-flop coupled EB system has not been systematically investigated. In this paper, we first reveal the role of bulk AFM structures on the spin reorientation transition using a series of $Fe_{(FM)}/MnPd_{(AFM)}$ bilayer samples of varying AFM thicknesses. We also studied the effective change in the internal AFM spin configuration and its role in EB by FM reversal using well-behaved, epitaxially grown multilayer samples, i.e., $Fe_{(FM1)}/MnPd_{(AFM1)}/Fe_{(FM2)}/IrMn_{(AFM2)}$. In this multilayer structure, AFM1 is the *a* axis MnPd that has a blocking temperature, $T_B^{MnPd}$, ~90 K.[9] AFM2 is IrMn with $T_B^{IrMn} >$ RT, which is used to provide a strong pinning on FM2. This enables us to define the AFM1 bulk spin arrangement at room temperature (RT) by field-cooling FM1 and FM2 in parallel (P) or antiparallel (AP) configurations. Observations of how the FM magnetization history in the FM2/AFM2 couple affects the EB of the FM1/AFM1 couple provide direct evidence for the specific role played by the bulk AFM spins, as a function of thickness, and how they rearrange during the magnetization switching of the individual FM layers on either side of the AFM1.

## II. EXPERIMENT

Epitaxial bilayers and multilayers were fabricated on the MgO(001) substrate by ion beam sputtering following our earlier works[18,19] and specifically the recipe in Ref. 9. Bilayer samples have a $Fe_{(100\,Å)}/a$ axis $MnPd_{(t\,Å)}$ structure with $t$ = 50, 100, 200, 300, 450, and 750 Å. Two multilayer samples have a $Fe_{(100\,Å)}/a$ axis $MnPd_{(s\,Å)}/Fe_{(100\,Å)}/IrMn_{(80\,Å)}$ stacking sequence with $s$ = 350 and 700 Å. Finally, all samples were protected by a 50-Å Ta capping layer. The multilayer sample structure is referred to as FM1/AFM1/FM2/AFM2 in all subsequent discussions. All samples were grown at 120 °C in the presence of an in-plane magnetic field, $H_{growth}$ = 300 Oe, along the Fe[100] easy direction to induce an exchange anisotropy only at the FM2/AFM2 interface. As a result, the FM2 layer is pinned and exhibits a loop shift at RT. Since the magnetizations of FM1 and FM2 switch at different fields, the effects of FM2 magnetization reversal on the EB of the FM1/AFM1 couple through the AFM1 bulk spin rearrangement can be readily detected. *M-H* curves were measured using a Quantum Design physical property measurement system over a wide temperature range from 10 to 300 K.

## III. RESULTS AND DISCUSSION

The bilayer samples were cooled from 300 to 20 K under a cooling field, $H_{cool}$ = 1 kOe P to $H_{growth}$ and subsequently measured at 20 K. We first used a large magnetic field of 1 kOe and cycled more than ten times to minimize the training effect of all layers. When $t$ < 300 Å, a conventional biased loop can be observed, and the $H_{eb}$ was determined by the center shift of the loop, Fig. 1(a). For samples with $t \geqslant$ 300 Å, a stepped loop can be observed indicating the low-temperature in-plane spin reorientation, Fig. 1(b). As in our previous study,[9] a shift field, $H_s$, was determined

 

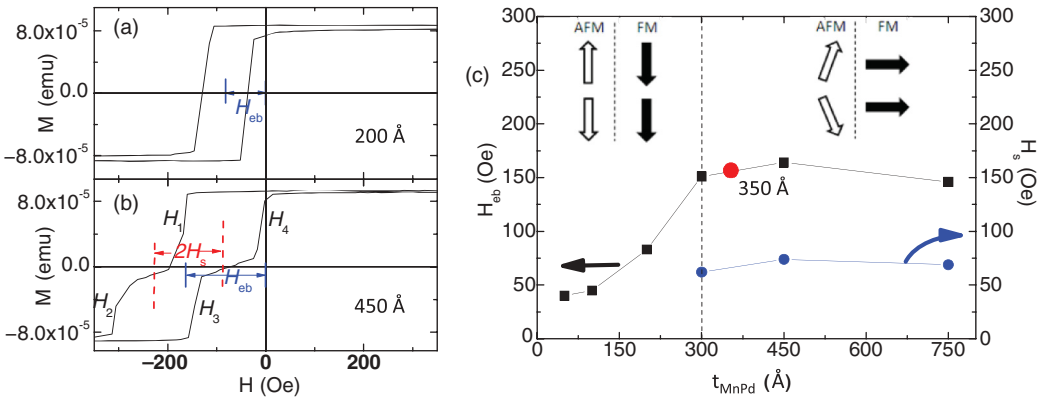


FIG. 1. (Color online) (a) Hysteresis loop of Fe/MnPd ($t$ = 200 Å) at 20 K. (b) Hysteresis loop of Fe/MnPd ($t$ = 450 Å) at 20 K. The determination of $H_s$ and $H_{eb}$ are illustrated. (c) Thickness dependence of $H_{eb}$ and $H_s$ of Fe/MnPd bilayer samples measured at 20 K. Interface coupling transitions from P to spin flop at $t_{sat} \sim 300$ Å.

from the center shift of the two subloops [Fig. 1(b)], i.e., $H_s = (H_1 - H_2 - H_3 + H_4)/4$, which is further related to a perpendicular $K_u$ via $K_u = M_s H_s$. $H_{eb}$ was determined by the center shift of the entire loop. The thickness dependence of $H_{eb}$ and $H_s$ were summarized in Fig. 1(c). $H_{eb}$ reached saturation at $t_{sat} = 300$ Å, which is also the critical thickness for the onset of $H_s$. The $t_{sat}$ is also understood as the maximum depth of the AFM spins in the bulk that can affect the interfacial coupling. It is very likely that such a length should be comparable to but not bigger than the longitudinal dimension, $\delta$, of stable AFM domains, which break the AFM long-range ordering.[16] Synchrotron and neutron experiments have also revealed the dimension of AFM domains to be around several tens of nanometers in epitaxial EB bilayers.[20] Such a large domain size is anticipated in epitaxial samples due to the well-defined chemical ordering. The longitudinal lattice constant for $a$ axis MnPd is ~3.94 Å,[18] so the width of a stable MnPd domain ($\delta \sim 300$ Å) contains ~76 atomic monolayers. This large $\delta$ in MnPd is unique, whereas much smaller values are usually observed in other AFMs such as IrMn ($\delta$~40 Å).[21] However, when the AFM layer thickness $> \delta$, no additional anisotropy energy is generated with increasing AFM thickness, and the EB is saturated. More detailed information on the AFM domains may be provided by synchrotron measurements.[22] Notably, the scenario here is different from polycrystalline EB bilayers, where the $t_{sat}$ is largely set by the dimension of much smaller AFM grains.[16]

In the FM1/AFM1/FM2/AFM2 multilayer sample with $s$ = 350 Å, the MnPd thickness is just enough to support a single, fully developed, AFM domain. Figure 2(a) shows the RT hysteresis curve for the $s$ = 350 Å sample measured along $H_{growth}$ after minimizing the training effect. The solid curve reflects the magnetization switching of the entire structure, containing two magnetization hysteresis subloops. Due to additional pinning in the FM2 layer, the upper and lower subloops should correspond to FM1 and FM2, respectively. The solid FM1 subloops reflect the FM1/AFM1 coupling with the FM2 magnetization experiencing a complete switching process, from being first aligned P to $H_{growth}$ to the opposite direction and then back to align with $H_{growth}$. In the same figure, the dashed lines correspond to the magnetization minor loops for FM1 without FM2 layer switching. In simple terms, the solid and dashed FM1 loops compare the FM1/AFM1 EB with and without a complete FM2 switching process. Notably, without switching of FM2, the ascending branch of the FM1 loop shifts leftward. For the other multilayer sample, $s \sim 700$ Å $> 2\delta$ [Fig. 2(b)], the effect of FM2 magnetization history is much less pronounced and almost indiscernible, indicating that the ascending branches of FM1 are not affected by the FM2 switching. These observations provide direct evidence that a nonrecoverable change in the AFM1 can occur during FM2 magnetization switching, i.e., the bulk AFM1 spin structure is affected by the FM2 magnetization configuration. When $s$ is comparable to $\delta$, the AFM1 spin rotation driven by the switching of FM1 and FM2 overlap with each other, which makes it possible to overcome the energy barrier of the spin configuration built by their initial state and partially unlock the EB of FM1 after switching FM2 back and forth.[17] However, when $s > 2\delta$, AFM1 spins from both interfaces to their respective bulk parts rotate independently; therefore, the switching of FM2 has no effect on FM1.

The effect of FM reversal on the AFM bulk spin structure was further investigated by field cooling the thin multilayer sample to $T < T_B^{MnPd}$ with FM1 and FM2 P or AP to each other. At $T < T_B^{MnPd}$, due to the spin-flop exchange coupling, shifted and stepped hysteresis loops can be simultaneously observed, Fig. 2(c). For P cooling, $H_{cool} = +20$ Oe was applied at RT, and the sample was subsequently cooled to 20 K and measured (solid curve). EB and spin reorientation behavior were observed for both FM1 and FM2 subloops. $H_S^{FM1} = (H_1 - H_2 - H_3 + H_4)/4 = 42$ Oe and $H_{eb}^{FM1} = -34$ Oe are obtained for FM1, and $H_S^{FM2} = (H_I - H_{II} - H_{III} + H_{IV})/4 = 50$ Oe and $H_{eb}^{FM2} = -174$ Oe are obtained for FM2. Note that $|H_{eb}^{FM2}| \gg |H_{eb}^{FM1}|$ due to the contribution from both AFM1/FM2 and FM2/AFM2 interfacial couplings. In the FM1 subloop, the field difference between the two sequential steps in the descending branch, i.e., $|H_1 - H_2| \sim 108$ Oe, is greater than that for ascending branch $|H_3 - H_4| \sim 61$ Oe. This is attributed to the propagation effect of the EB[23] that shifted $H_2$ leftward due to the P cooling of FM2 along the $H_{growth}$. Physically, it is harder to fully reverse FM1 to $-H_{growth}$ with FM2 cooled along $H_{growth}$.

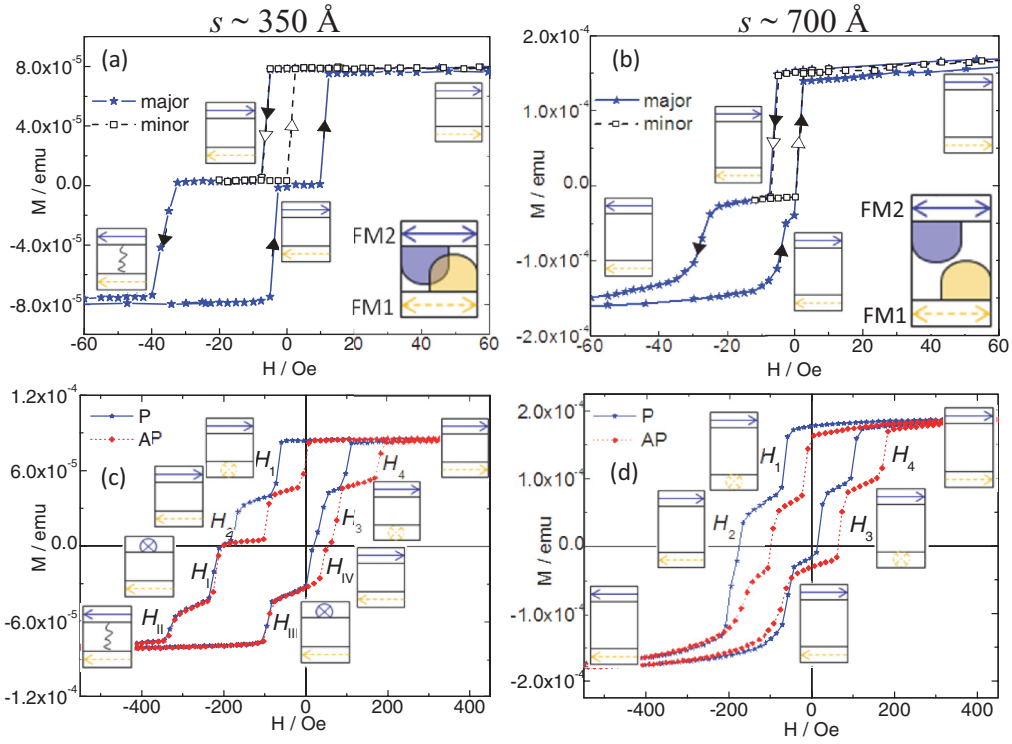


FIG. 2. (Color online) RT major and minor loops of (a) thin ($s \sim 350$ Å) and (b) thick ($s \sim 700$ Å) multilayer samples. Hysteresis loops measured at 20 K under P and AP cooling from RT of (c) thin ($s \sim 350$ Å) and (d) thick ($s \sim 700$ Å) multilayer sample. Magnetization configuration of FM1 (dashed arrow) and FM2 (solid arrow) are illustrated in an enclosed box for each magnetic switching.

For AP cooling, $H_{\text{cool}}$ is $-18$ Oe, approached from a large positive field, to reverse only FM1; the whole structure is subsequently cooled to 20 K and measured (dashed curve). The FM2 subloop looks almost the same with the P cooling configuration; however, the FM1 subloop shifts to the positive field direction. Thus, $H_S^{\text{FM1}} = 44$ Oe and $H_{\text{eb}}^{\text{FM1}} = 36$ Oe are obtained from the FM1 subloop. Similarly, $H_{\text{IV}}$, also shifts towards the positive field direction due to the EB propagation effect. Physically, FM1 is now pinned along $-H_{\text{growth}}$, which makes it harder for FM2 to reverse back to $H_{\text{growth}}$. On the other hand, the FM1 subloop is symmetric with respect to its center in the AP case, i.e., $|H_1 - H_2| \sim 96$ Oe and $|H_3 - H_4| \sim 103$ Oe.

Figure 2(d) compared the hysteresis loops for the other multilayer sample in the two field-cooling configurations. FM1 spin reorientation can be clearly observed, as indicated by the stepped FM1 subloop. However, such behavior is missing for the FM2 layer, which indicates that the spin-flop coupling was not maintained throughout the MnPd layer. For this sample with $s$ (700 Å) $>2\delta$, during sample growth, the bulk AFM stabilizes at least two separated, fully developed domains, located at the FM1/AFM1 and AFM1/FM2 interfaces, respectively. Therefore, the spin-flop coupling established at the FM1/AFM1 interface can only propagate within its respective domain but is stopped at any domain wall (DW). From Fig. 2(d), $H_S^{\text{FM1}} = 46$ Oe and $H_{\text{eb}}^{\text{FM1}} = -28$ Oe, for the P cooling configuration, and $H_S^{\text{FM1}} = 45$ Oe and $H_{\text{eb}}^{\text{FM1}} = 30$ Oe, for the AP case, were obtained.

The minor loop at each distinct reversal step for the descending branch were further studied to reveal spin-flop coupling and the effect of the bulk AFM structure, Fig. 3. Samples were first cycled under large magnetic field (1 kOe) to minimize training effects. As discussed earlier, $H_1$ points to the spin reorientation of FM1, in which the magnetization is along Fe[010], perpendicular to $H_{\text{growth}}$. The associated minor loop, $M_1$, is irreversible for both cooling configurations [Figs. 3(a) and 3(b)], showing that magnetic switching is mainly via DW nucleation and propagation.[24] The second minor loop, $M_2$, represents the complete FM1 hysteresis subloop with FM2 kept fixed along $H_{\text{growth}}$. For P cooling, for FM1, the switching field shifts leftward upon reversal back from negative field direction to the reoriented state, Fe[010], when compared to the subloop for the full hysteresis (solid). However, for AP cooling, $M_2$ show almost indiscernible difference with the full hysteresis subloop. The result indicated that the internal AFM1 domain structure depends on the cooling process as well as the reversal history. In the P configuration, nonrecoverable change in the AFM1 occurs at $H_{\text{II}}$ when both FM1 and FM2 were reversed from their original cooled stable states. In such circumstances, when a FM domain is reversed, the adjacent AFM spin structure is exposed to a magnetic torque whose magnitude is given by the strength of the FM/AFM exchange coupling. A strong torque exerted from both FM1 and FM2 when combined positively is able to alter the internal AFM1 spin structure. In the AP case, however, AFM1 is subjected to one torque (by FM2) and to another torque (by FM1) in the descending and ascending branches. A single torque exerted on the AFM at any one time is not strong enough to bring about nonrecoverable changes in the AFM. In addition, the AP cooling mode forced the formation of at least two AP

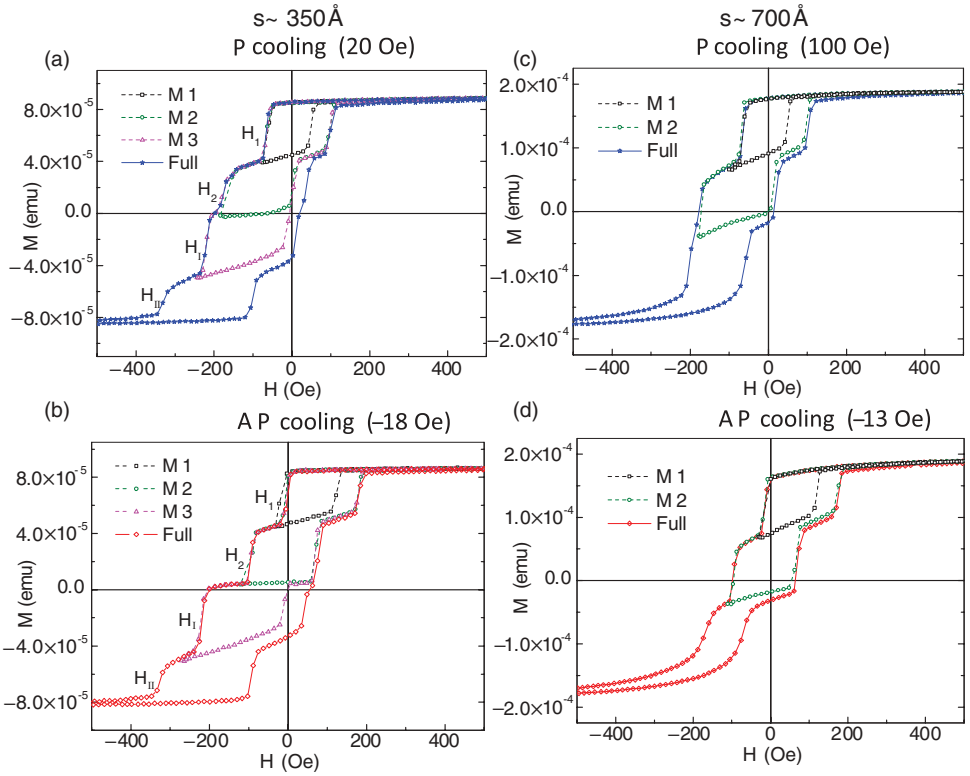


FIG. 3. (Color online) Complete hysteresis (solid) and minor loops (open) measured at 20 K for (a) P cooling and (b) AP cooling of the thin multilayer sample. Complete hysteresis (solid) and minor loops (open) measured at 20 K for (c) P cooling and (d) AP cooling of the thick multilayer sample.

AFM domains in the bulk, one at each FM interface.[13] Thus, this torque exerted on the AFM, from either FM1 or FM2, was absorbed within each respective AFM domain, and any long-range spin effects are not able to propagate across the DW. As a result, the spin states of FM1 and FM2 are not able to influence each other through the bulk AFM spins. This is an elegant experimental demonstration of the effect of FM reversal on bulk AFM spin structure.

It is worth noting that the perpendicular reoriented state causes no effect on the AFM bulk spin structure, as revealed by minor loop $M_3$. Specifically, FM2 switched to the reoriented state at $H_I$ and then irreversibly switched back to $H_{growth}$, but the FM1 subloop in $M_3$ showed indiscernible difference compared with $M_2$. It is likely because the spin-flop coupling only gives rise to an effective uniaxial anisotropy, which reorients the FM magnetization by DW nucleation and propagation. The DW movement along the intermediate reoriented state effectively introduces a lower torque on the AFM and has only a small effect on the bulk domain structures that control the EB. Similar measurements were conducted for the sample with $s = 700$ Å, under P [Fig. 3(c)] and AP [Fig. 3(d)] cooling mode. In both cooling modes, the minor loop $M_2$ is indiscernible from the full hysteresis subloop, which indicates that the AFM spins at the FM1/AFM1 and AFM1/FM2 interfaces, including their respective inner parts, do not communicate due to the thick AFM layer.

Further temperature-dependent measurements indicate that the spin reorientation and EB can be simultaneously observed up to ~50 K. $|H_{eb}(T)|$ and $H_s(T)$ for FM1 of the thin multilayer sample ($s = 350$ Å) under both cooling modes are summarized in Fig. 4(a). $H_s$ showed the same temperature behavior as $|H_{eb}|$. The strong correlation in the temperature dependence of $H_s$ and $H_{eb}$ confirms that the spin-flop coupling is attributable for the EB. For AP cooling, both $|H_{eb}|$ and $H_s$ decay with temperature from 10 to 40 K. However, for P cooling, $|H_{eb}|$ and $H_s$ are suppressed and maintained a constant value at low temperatures from 10 to 20 K. Unlike the collinear-coupled system,[13] the spin-flop-coupled EB value is more significant in the AP cooling case at low temperatures.

To interpret our observations, we propose a qualitative model based on spin-flop coupling [Fig. 4(c)]. Such a model does not rely on complex AFM spin structures but only on simple assumptions, i.e., possible AFM domain formation[13,25] and the interfacial spin canting[9] at different depths within the AFM. An AP configuration of FM1 and FM2 can mutually drag the AFM spins to the perpendicular direction (large rotating angles) thus favoring the perpendicular spin-flop coupling and leading to a greater $H_s$; besides, it also assists the formation of opposite frozen-in domains and associated DWs in the AFM bulk.[13] Uncompensated AFM moments can be enhanced by the DW passing through the defects or dislocations in the films and thus increase the $H_{eb}$ according to the domain state model.[11,17,26,27] On the contrary, P cooled FM1 and FM2, both along $H_{growth}$, will favor the competing P spin coupling with small rotating angles throughout the AFM bulk; this P configuration also decreases the possibility for AFM DW formation. As a result, both $|H_{eb}|$ and $H_s$ are suppressed when compared with the AP cooling configuration at low temperatures. Our model qualitatively explains the differences for P and AP cooling configurations. Besides, it also sheds light on tuning the spin-flop coupling via the extrinsic, field-cooling approach in epitaxial samples.

A similar effect has been observed at the AFM1/FM2 interface. As shown, in Fig. 4(b), a gap of $H_s$ at 10 ~ 20 K was

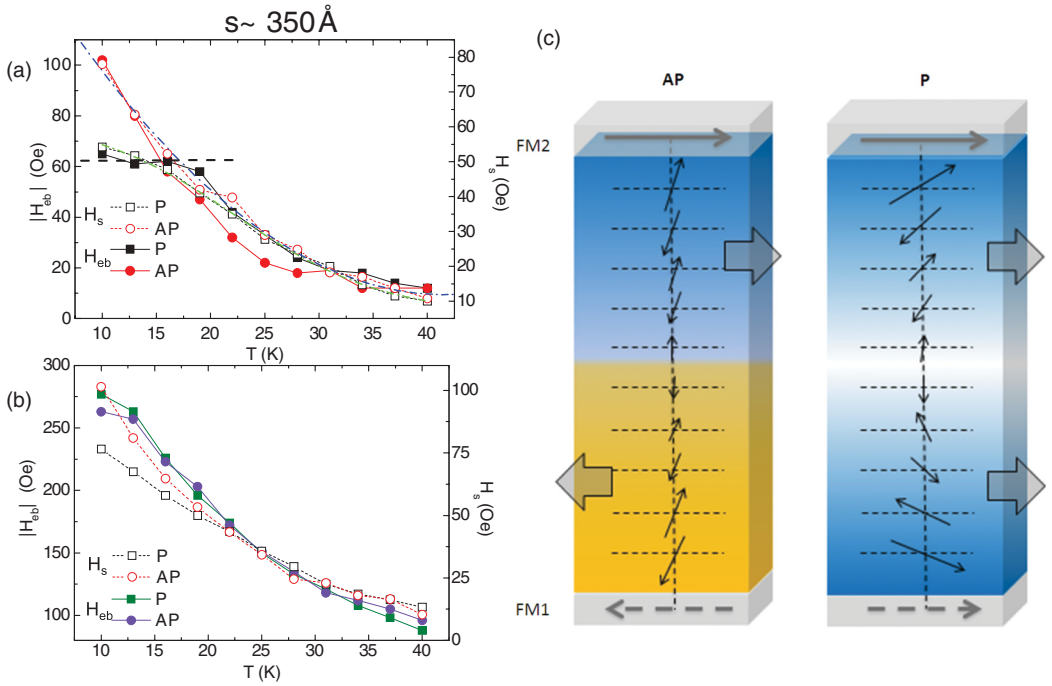


FIG. 4. (Color online) (a) Temperature dependence of $|H_{eb}|$ (solid) and $H_s$ (open) under P (square) and AP (circle) cooling process of FM1. Two lines (in dash dot) are a guide to the eye. (b) Temperature dependence of $|H_{eb}|$ (solid) and $H_s$ (open) under P (square) and AP (circle) cooling process of FM2. (c) Schematic illustration of a qualitative model, showing the possible AFM domain formation and spin canting for the two cooling modes. Block arrows indicate the preferred canting directions at different regions in the AFM.

found between the P and AP cooling mode. $|H_{eb}|$ decreases with temperature and almost overlaps each other for P and AP cooling configurations, due to the much stronger pinning of FM2 by the AFM2 from the other interface. Finally, note that measurements for the thick multilayer sample showed almost overlapped behavior of $|H_{eb}|$ and $H_s$ of FM1 and $|H_{eb}|$ of FM2 (not shown), confirming the noninteracting interfaces on the two sides of thick AFM.

## IV. CONCLUSIONS

In summary, we have revealed the role of bulk AFM structures on the EB with the spin reorientation transitions in epitaxial bilayers and multilayers. The large correlation length of the order of ~300 Å for the epitaxial AFM, MnPd, was confirmed. Using such multilayered sandwich structures, the effect of FM magnetization history on the bulk AFM spins are elegantly investigated at both the saturated (final) and the spin-reoriented (intermediate) FM states. The saturated FM state, achieved by magnetization rotation, is considered the relevant process for the effective AFM bulk modification, due to the exertion of a larger spin torque, as compared with the spin-reoriented state that only involves ferromagnetic DW movement.

## ACKNOWLEDGMENT

This work was supported by NSF/DMR No. 1063489.

*Corresponding author: kannanmk@uw.edu

[1]W. H. Meiklejohn and C. P. Bean, Phys. Rev. **102**, 1413 (1956).
[2]J. Nogués and I. K. Schuller, J. Magn. Magn. Mater. **192**, 203 (1999); A. E. Berkowitz and K. Takano, *ibid.* **200**, 552 (1999); R. L. Stamps, J. Phys. D **33**, R247 (2000).
[3]P. Blomqvist, K. M. Krishnan, and H. Ohldag, Phys. Rev. Lett. **94**, 107203 (2005).
[4]S. Bruck, G. Schutz, E. Goering, X. Ji, and K. M. Krishnan, Phys. Rev. Lett. **101**, 126402 (2008).
[5]M. Kiwi, J. Magn. Magn. Mater. **234**, 584 (2001).
[6]N. C. Koon, Phys. Rev. Lett. **78**, 4865 (1997).
[7]T. C. Schulthess and W. H. Butler, Phys. Rev. Lett. **81**, 4516 (1998).
[8]T. J. Moran, J. Nogues, D. Lederman, and Ivan K. Schuller, Appl. Phys. Lett. **72**, 617 (1998).
[9]Q. F. Zhan and K. M. Krishnan, Appl. Phys. Lett. **96**, 112506 (2010).
[10]A. Barbier, C. Mocuta, W. Neubeck, M. Mulazzi, F. Yakhou, K. Chesnel, A. Sollier, C. Vettier, and F. de Bergevin, Phys. Rev. Lett. **93**, 257208 (2004).
[11]U. Nowak, K. D. Usadel, J. Keller, P. Miltenyi, B. Beschoten, and G. Guntherodt, Phys. Rev. B **66**, 014430 (2002).
[12]G. Malinowski, M. Hehn, S. Robert, O. Lenoble, A. Schuhl, and P. Panissod, Phys. Rev. B **68**, 184404 (2003).
[13]R. Morales, Z. P. Li, J. Olamit, K. Liu, J. M. Alameda, and I. K. Schuller, Phys. Rev. Lett. **102**, 097201 (2009).
[14]F. Y. Yang and C. L. Chien, Phys. Rev. Lett. **85**, 2597 (2000).
[15]M. G. Blamire, M. Ali, C. W. Leung, C. H. Marrows, and B. J. Hickey, Phys. Rev. Lett. **98**, 217202 (2007).

[16]K. O'Grady, L. E. Fernandez-Outon, and G. Vallejo-Fernandez, J. Magn. Magn. Mater. **322**, 883 (2010).
[17]Y. Xu, Q. Ma, J. W. Cai, and L. Sun, Phys. Rev. B **84**, 054453 (2011).
[18]N. Cheng, J.-P. Ahn, and K. M. Krishnan, J. Appl. Phys. **89**, 6597 (2001).
[19]P. Blomqvist, K. M. Krishnan, and D. E. McCready, J. Appl. Phys. **95**, 8019 (2004).
[20]F. Radu, S. K. Mishra, I. Zizak, A. I. Erko, H. A. Durr, W. Eberhardt, G. Nowak, S. Buschhorn, H. Zabel, K. Zhernenkov, M. Wolff, D. Schmitz, E. Schierle, E. Dudzik, and R. Feyerherm, Phys. Rev. B **79**, 184425 (2009).
[21]M. Ali, C. H. Marrows, M. Al-Jawad, B. J. Hickey, A. Misra, U. Nowak, and K. D. Usadel, Phys. Rev. B **68**, 214420 (2003).
[22]G. Srajer, L. H. Lewis, S. D. Bader, A. J. Epstein, C. S. Fadley, E. E. Fullerton, A. Hoffmann, J. B. Kortright, Kannan M. Krishnan, S. A. Majetich, T. S. Rahman, C. A. Ross, M. B. Salamon, I. K. Schuller, T. C. Schulthess, and J. Z. Sun, J. Magn. Magn. Mater. **307**, 1 (2006).
[23]D. N. H. Nam, W. Chen, K. G. West, D. M. Kirkwood, J. Lu, and S. A. Wolf, Appl. Phys. Lett. **93**, 152504 (2008).
[24]Q. F. Zhan and K. M. Krishnan, J. Appl. Phys. **107**, 09D703 (2010).
[25]D. Mauri, H. C. Siegmann, P. S. Bagus, and E. Kay, J. Appl. Phys. **62**, 3047 (1987).
[26]Q. F. Zhan, W. Zhang, and K. M. Krishnan, Phys. Rev. B **83**, 094404 (2011).
[27]P. Miltenyi, M. Gierlings, J. Keller, B. Beschoten, G. Guntherodt, U. Nowak, and K. D. Usadel, Phys. Rev. Lett. **84**, 4224 (2000).